

## Influence of Water Adsorption on Electrochemical Performance of Plasma Modified MCMB Powders

H. Tanaka\*, Y. Moriyoshi\*, M. Kurihara\*\*, S. Maruyama\*\* and T. Ishigaki\*\*\*

\*Hosei University, Department of Materials Science, 3-7-2 Kajino-cho, Koganei-shi, Tokyo 184-8584, Japan

Fax: 81-29-860-4701, e-mail: TANAKA.Hideki@nims.go.jp

\*\*TDK Corp., R & D Center, 2-15-7 Higashi-Owada, Ichikawa-shi, Chiba 272-8558,

Fax: 81-47-378-9178, e-mail: mk@mb1.tdk.co.jp

\*\*\*National Institute for Materials Science, Advanced Materials Laboratory,

1-1 Namiki, Tsukuba-shi, Ibaraki 305-0044, Japan,

Fax: 81-29-860-4701, e-mail: ISHIGAKI.Takamasa@nims.go.jp

Mesocarbon microbeads (MCMB) powders, which are known to be highly crystallized carbon materials and have a mean particle size of 11 $\mu$ m, were treated in RF thermal plasmas. Through the plasma treatment, the surface morphology, structure, and chemical composition of the powder were modified. The plasma-induced modification made the surface of MCMB particles disordered, i.e. the improvements in the thermal stability and electrochemical properties of the powders, such as the discharge capacity and first charge/discharge efficiency as an anode in lithium-ion rechargeable batteries. Powders obtained without air exposure showed further improvement in electrochemical performance as anode materials.

Key words: MCMB, Thermal plasma treatment, Electrochemical property, Thermal stability, Lithium-ion rechargeable battery.

### 1. INTRODUCTION

Carbonaceous materials have been investigated extensively as an anode material of lithium-ion rechargeable battery because they have high discharge capacity, low electrode potential, high charge/discharge efficiency, long cycle life, and high level of safety. The discharge capacity and first charge/discharge efficiency are the most important electrode characteristics. The first charge/discharge efficiency decreases with the irreversible capacity increase. Irreversible capacity originates from the formation of a protective film on the graphite surface called "solid electrolyte interphase" (SEI) and other irreversible side reactions. The SEI composition and properties strongly depend on the electrolyte and surface properties of the graphite electrode, and the formation of SEI causes a decrease in the first charge/discharge efficiency.

Another important characteristic is the thermal stability of lithium-ion rechargeable batteries. The onset temperature of the exothermic reactions strongly depends on SEI components, therefore the SEI components influence the thermal stability of graphite anode.

RF thermal plasma has great advantages in material modification and chemical reactions, because of its high temperature and active species in it. Many kinds of materials with unique properties have been prepared by RF thermal plasma processes [1-3]. Plasma-treated carbon powders were modified in chemical composition and surface morphology. The modifications led to a higher capacity than that of untreated powders when the powders were used as an anode in lithium-ion rechargeable batteries.

In this study, mesocarbon microbeads (MCMB) powders were modified by RF thermal plasmas in an attempt to improve the electrochemical properties of the MCMB powders as anode materials in Lithium-ion

rechargeable battery. The electrochemical properties of the plasma-treated powder and the effect of water-vapor adsorption on its surface on the electrochemical properties were investigated from the viewpoint of using the powder as an anode in lithium-ion rechargeable batteries. We discuss the thermal stability of the plasma-treated MCMB powders and how plasma treatment affects the passivating quality of the SEI.

### 2. EXPERIMENTS

The RF thermal plasma torch and reactor chamber used in the present study have been reported elsewhere [1]. The raw materials were MCMB powders with mean particle size of 11  $\mu$ m (MCMB 10-28, Osaka Gas Co.). MCMB powder granules, a sort of artificial graphite that is highly graphitized and composed of lamella graphite grains, are spherical, and the powder has a 99.9% or more carbon content. The powder was treated in Ar-H<sub>2</sub>, Ar-N<sub>2</sub>, Ar-H<sub>2</sub>-CO<sub>2</sub>, and Ar-N<sub>2</sub>-CO<sub>2</sub> RF thermal plasmas at 27 kPa generated at a plate power level of 40 kW. The powder-feed rate was adjusted to 17 g/min, at which rate the optimal conditions for heating the powders were attained. To avoid the exposure in air, i.e., adsorption of water vapor, during the collection procedure, the plasma-treated powders were collected in argon atmosphere, while the powders were usually collected in air. The plasma generating and powder feeding conditions are summarized in Table I.

The powders were observed by scanning electron microscopy (SEM, JEOL, JSM-5410) to characterize their surface morphologies, and by X-ray diffractometry (XRD) to identify the bulk structure formed through the thermal-plasma treatment. Several-nanometer-deep crystallinity was observed on the surface by Raman scattering spectroscopy (JASCO, NR-1800). The Brunauer-Emmett-Teller (BET) surface area was also

Table I Plasma generating and powder feeding condition.

| Sample                         | a                 | b                    | c                 | d                    |
|--------------------------------|-------------------|----------------------|-------------------|----------------------|
| Plasma gas / l/min             | Ar/15             | Ar/15                | Ar/15             | Ar/15                |
| Sheath gas (1) / l/min         | Ar/60             | Ar/60                | Ar/60             | Ar/60                |
| Sheath gas (2) / l/min         | H <sub>2</sub> /3 | H <sub>2</sub> /3    | N <sub>2</sub> /3 | N <sub>2</sub> /3    |
| Powder carrier gas (1) / l/min | Ar/10             | Ar/9.5               | Ar/10             | Ar/9.5               |
| Powder carrier gas (2) / l/min |                   | CO <sub>2</sub> /0.5 |                   | CO <sub>2</sub> /0.5 |
| R.F. Frequency / MHz           |                   | 4                    |                   |                      |
| Plate power / kW               |                   | 40                   |                   |                      |
| Reactor pressure / kPa         |                   | 27                   |                   |                      |
| Powder feed rate / g/min       |                   | 17                   |                   |                      |

measured (BEL JAPAN, BELSORP18). The contents of oxygen, nitrogen, and hydrogen were measured by an oxygen/nitrogen analyzer (Horiba, EMGA-650) and a hydrogen analyzer (Horiba, EMGA-621), respectively. The adsorption species on the surface of the powders were analyzed using thermal desorption spectroscopy (TDS: ESCO EMD-WA1000).

Electrochemical measurements of the powders as an anode for lithium-ion rechargeable batteries were performed in non-aqueous solvents containing 1M LiClO<sub>4</sub>. Sample electrodes were prepared to examine the anode properties for lithium-ion rechargeable batteries as follows: Polyvinylidene fluoride used as a binder and a slurry were spread on a copper foil and dried at 150°C under vacuum for one hour; a 1 mol/cm<sup>3</sup> solution of LiClO<sub>4</sub> in a 50:50 mixture of ethylene carbonate (EC) and diethyl carbonate (DEC) was used as an electrolyte; a counter lithium electrode and a reference lithium electrode were used; an electrochemical cell was set up in a dry box under argon atmosphere, and the charge/discharge behavior of the cell was measured galvanostatically at a current density of 0.25 mA/cm<sup>2</sup> between 0 and 3 V vs. Li/Li<sup>+</sup> at 25°C.

To determine the thermal stability, the thermal decomposition reactions of the lithiated graphite anode with the electrolyte solution were examined by differential scanning calorimetry (DSC: RIGAKU Thermo Plus DSC 8239L). DSC scans were carried out at a heating rate of 10 °C/min, in the temperature range from the room temperature to 400°C, in an argon-gas-filled sample case.

### 3. RESULTS AND DISCUSSION

The lattice parameter of the plasma-treated and original MCMB powders was determined to be  $d_{002}=0.336$  nm by XRD. The crystalline particle sizes in the c-direction ( $L_c$ ) and a-direction ( $L_a$ ) of the

plasma-treated powders were 32 and 63 nm, respectively, which were also the same as those of the original powders. The plasma-treated powders did not show any further graphitization in the bulk. However, surface on the plasma-treated MCMB particles can be recognized to change into more disordered structure judging from Raman spectra. Thus the surface layer of original MCMB was removed and displaced by new layer through plasma treatment.

Figure 1 shows the typical morphology obtained from the original and plasma-treated MCMB powders. The Ar-H<sub>2</sub> plasma-treated powder had a surface morphology that was covered with fine particles several tens of nanometers in size. The MCMB powders were heated and partially evaporated. The evaporation was followed by the formation of nano-size condensate through coagulation from a vapor phase during cooling, and the condensate covered the surface of the coarse particles. The Ar-H<sub>2</sub>-CO<sub>2</sub> plasma-treated powder shown in Fig. 1(c) had a rough surface. In the Ar-H<sub>2</sub>-CO<sub>2</sub> plasma treatment, the evaporated species were almost completely burned off by oxygen atoms, which formed concurrently as a result of the decomposition of CO<sub>2</sub>. The surface was chemically etched, and a lamellae structure peculiar to MCMB was revealed on the surface. The Ar-N<sub>2</sub> and Ar-N<sub>2</sub>-CO<sub>2</sub> plasma-treated powders also showed similar tendency.

The BET surface areas of the Ar-H<sub>2</sub>, Ar-N<sub>2</sub>, Ar-H<sub>2</sub>-CO<sub>2</sub>, and Ar-N<sub>2</sub>-CO<sub>2</sub> plasma-treated MCMB powders were 1.87, 2.01, 1.31, and 1.62 m<sup>2</sup>/g, respectively, while the value for the original powder was 1.83. The BET surface area changed with plasma atmospheres, and it corresponded to the variation in the surface morphology.

The plasma-treated powders showed a unique variation in their chemical composition. The hydrogen, oxygen, and nitrogen contents induced by the plasma treatment changed with the composition of the plasma. In all plasma treatments, both the hydrogen and oxygen contents increased. In particular, the content of nitrogen in the Ar-N<sub>2</sub> plasma-treated powder was five times larger than that in the original powder.

To determine the surface compositions of hydrogen, oxygen and nitrogen in the plasma-treated powders, the plasma-treated powders were examined by thermal desorption spectroscopy (TDS). The evolved gases were H<sub>2</sub>, CH<sub>4</sub>, H<sub>2</sub>O, CO, and CO<sub>2</sub> in all the plasma-treated powders, and NH<sub>3</sub> was detected in the powders treated in the atmospheres containing N<sub>2</sub>.

Figure 2 shows the TDS spectra of the original and plasma-treated MCMB powders for H<sub>2</sub> ( $M/e=2$ ), H<sub>2</sub>O ( $M/e=18$ ) and CO<sub>2</sub> ( $M/e=44$ ) desorbed from the surface.

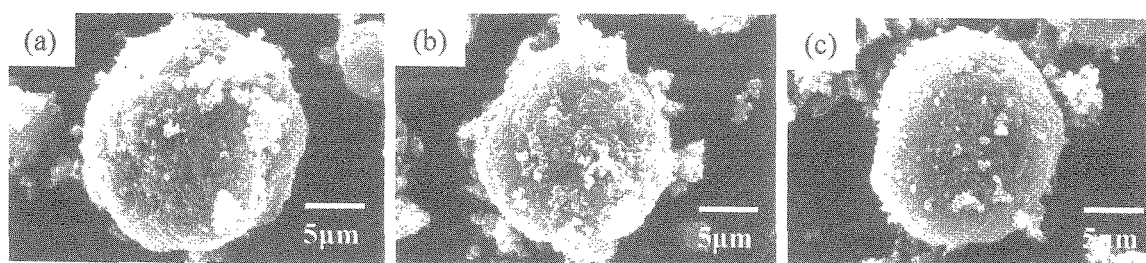


Fig.1 Surface morphology of the (a) original and (b), (c) plasma-treated MCMB powders: (b) Ar-H<sub>2</sub> plasma, (c) Ar-H<sub>2</sub>-CO<sub>2</sub> plasma.

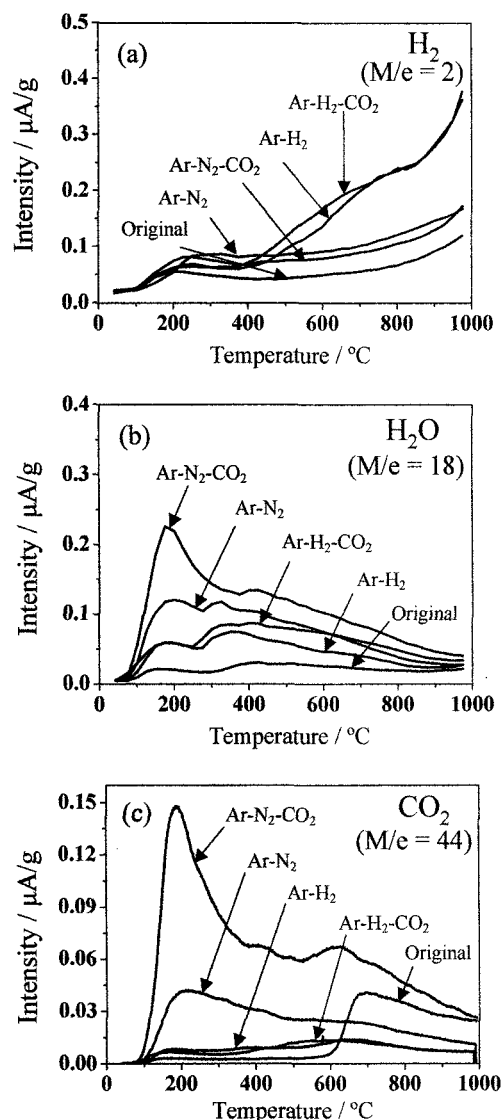


Fig.2 TDS spectra obtained from the original and plasma-treated MCMB powders: (a)  $\text{H}_2$  ( $M/e=2$ ), (b)  $\text{H}_2\text{O}$  ( $M/e=18$ ), and (c)  $\text{CO}_2$  ( $M/e=44$ ).

In the TDS of  $\text{H}_2\text{O}$ , the content of desorbed  $\text{H}_2\text{O}$  increased because the plasma treatment created a new active surface, which easily adsorbed  $\text{H}_2\text{O}$ . There was a remarkable peak of  $\text{H}_2$  at a relatively high temperature (more than  $500^{\circ}\text{C}$ ) in the powders treated in the atmospheres containing  $\text{H}_2$ . The appearance of out-gassed  $\text{CO}_2$  was due to the decomposition of the samples, not the desorption of the physical adsorption. This result indicates that the surface layer and the underneath of the surface were modified by reactive plasmas including  $\text{CO}_2$ . The content of desorbed hydrogen, oxygen, and nitrogen molecules calculated from the TDS results agreed with that calculated using elemental analysis. This result suggests that all the changes in the chemical composition took place predominantly in the surface region.

The first charge/discharge efficiency and the discharge capacity are typical important values in terms of battery performance. The first charge/discharge

efficiency of the original and  $\text{Ar-H}_2$ ,  $\text{Ar-N}_2$ ,  $\text{Ar-H}_2\text{-CO}_2$ , and  $\text{Ar-N}_2\text{-CO}_2$  plasma-treated powders was 90.3, 91.5, 91.2, 91.4 and 91.6%, respectively. The difference in the surface structure affected the first charge/discharge efficiency. It is remarkable that the plasma treatment improved the first charge/discharge efficiency. In the powder treated in the  $\text{Ar-N}_2\text{-CO}_2$ , the first charge/discharge efficiency was much improved. The first charge/discharge efficiency showed a tendency to decrease with an increase in the surface area because of the capacity loss by the side reactions, which are believed to form a SEI on the surface of graphite [4]. Thus, the increase of first charge/discharge efficiency of the  $\text{Ar-N}_2$  plasma-treated powder was smaller.

The relative discharge capacity of the  $\text{Ar-H}_2$ ,  $\text{Ar-N}_2$ ,  $\text{Ar-H}_2\text{-CO}_2$ , and  $\text{Ar-N}_2\text{-CO}_2$  plasma-treated powders were 109, 108, 107 and 105, respectively (the discharge capacity of the original was set to be 100). As a result, the plasma treatment gave rise to a 5–9% increase in the discharge capacity. Mabuchi and colleagues have reported that in heat-treatment processes at  $2000^{\circ}\text{C}$  or higher, the discharge capacity of MCMB powder shows a tendency to increase with an increase in the heat-treatment temperatures [5]. It is believed that at temperatures higher than  $2000^{\circ}\text{C}$ , the interlayer spacing,  $d_{002}$ , between the graphite layers, approaches a fixed value of 3.354  $\text{\AA}$ , and the crystal growth proceeds on the graphite layers in the direction of the C axis and then spreads in the direction of the A axis. Therefore, any increase in the charge/discharge capacity depends on the stacking and spreading of the graphite layers. Since no significant difference was found using XRD before and after the plasma treatment, there may have been no growth of the graphite crystals. The surface characteristics of the plasma-treated powders must be investigated further to properly clarify this mechanism.

In order to recognize the effect of adsorbed species, especially of water vapor, on the surface of MCMB powders, plasma-treated MCMB powders without exposure to air were prepared. The samples were collected in argon atmosphere in order to eliminate the adsorption of water vapor. The first charge/discharge efficiency was measured for the plasma-treated powders obtained without air exposure. The results of the first charge/discharge efficiency of the MCMB powders obtained without air exposure and that of the MCMB powders exposed to air are summarized in Fig.3. All the powders obtained without air exposure showed higher first charge/discharge efficiency than the exposed powders to air. The irreversible capacity of the MCMB powders obtained without air exposure decreased by 20–40%. Especially, in the  $\text{Ar-H}_2$  plasma treatment, the irreversible capacity was almost half as that of the original powder, which means 95% in the first charge/discharge efficiency. A general interpretation of this result is that the irreversible capacity of lithium ion intercalation into the graphite electrode during the first few cycles is associated with the formation of SEI film; therefore, it appears that surface properties greatly affect the irreversible capacity.

The properties of a graphite surface determine the thermal stability of lithium-ion rechargeable batteries. Maleki et al. have reported the thermal stability of

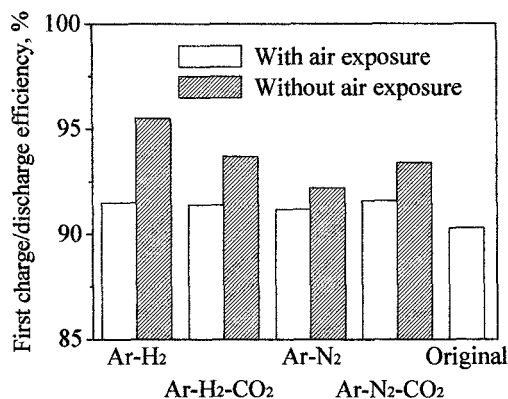


Fig.3 Effect of air exposure (especially, water vapor) on first charge/discharge efficiency.

carbonaceous materials used in lithium-ion rechargeable batteries showed three exothermic reaction peaks in the temperature range from 60 to 350°C in DSC [6]. The initial peak observed between 120 and 140°C is assigned to the decomposition of the SEI that forms on every carbonaceous material used in lithium-ion rechargeable batteries. The SEI is thought to be composed of metastable and stable components, and the initial peak is believed to be related to the transformation from metastable to stable components. On further heating, the lithiated carbon reacts with the molten polymer binder (most commonly, polyvinylidene difluoride, PVDF) at temperatures close to 200°C. The exothermic reactions at temperatures below 260°C are related to the breakdown of the SEI layer and electrolyte decomposition. Above 260°C, the major reactions are between Li<sub>x</sub>C<sub>6</sub> and PVDF.

Figure 4 shows a typical DSC curve of lithiated plasma-treated MCMB powder with electrolyte and binder. The DSC curve shows a mild heat generation beginning at 140°C, with a broad peak (peak 1). This mild heat generation continues until a sharp exothermic peak appears at 320°C (peak 3). The heat generations are attributed to the SEI layer formation and the electrolyte decomposition, and the reactions of products with lithiated plasma-treated MCMB powder and binder, respectively. The peak 1 is caused by a simple heterogeneous reaction between the electrolyte solvent and the lithiated graphite, which produces a passivating film on the carbon surface [7]. In other words, this mild heat generation is a result of a reaction between the lithiated graphite and the electrolyte to form a new SEI. Table II shows the amount of heat generated by the SEI reaction in the original and plasma-treated MCMB powders. Although the Ar-N<sub>2</sub> plasma-treated powder generated more heat per weight than the original powder did, the amount of heat generated per surface area by the plasma-treated powders decreased. From these results, we can see that the plasma treatment created a surface conducive to SEI formation.

#### 4. SUMMARY

MCMB powders were treated in various RF thermal plasmas. The plasma treatment made the surface of MCMB powder particles disordered, and gave rise to larger particles and unique chemical composition. The

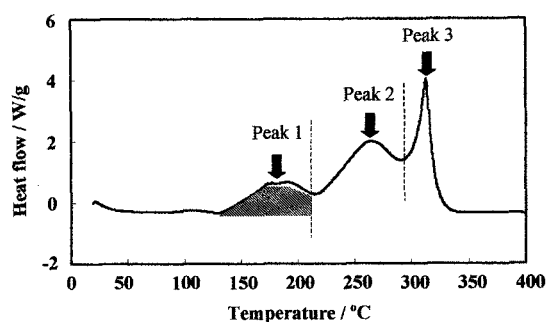


Fig.4 DSC curve of fully lithiated plasma-treated MCMB powder, electrolyte solution: 1M LiClO<sub>4</sub>/EC+DEC(3:7)

Table II Heat generation in SEI reaction of the original and plasma-treated MCMB powders.

| Sample                                    | Heat generation / J/g | J/m <sup>2</sup> |
|---|-----------------------|------------------|
| Original                                  | 314                   | 172              |
| Plasma treatment                          |                       |                  |
| Ar-H <sub>2</sub> plasma                  | 294                   | 132              |
| Ar-N <sub>2</sub> plasma                  | 402                   | 86               |
| Ar-H <sub>2</sub> -CO <sub>2</sub> plasma | 279                   | 144              |
| Ar-N <sub>2</sub> -CO <sub>2</sub> plasma | 234                   | 147              |

surface morphology, and chemical composition of the powders were found to be strongly dependent on the plasma composition. The plasma treatment improved the electrochemical properties of the powders such as the discharge capacity and first charge/discharge efficiency, and the thermal stability of the reaction for the SEI formation. The plasma treatment followed by an intentional post treatment, which eliminated the adsorption of water vapor on the surface of the powders, further improved their electrochemical properties. These results demonstrate that plasma treatment with adjusted plasma composition results in excellent electrochemical properties of MCMB powder when used as an anode in lithium-ion rechargeable batteries

#### REFERENCES

- [1] T. Ishigaki, Y. Moriyoshi, T. Watanabe, and A. Kanzawa, *J. Mater. Res.*, **11**, 2811-2824 (1996).
- [2] Y.L. Li and T. Ishigaki, *J. Am. Ceram. Soc.*, **84**, 1929-1936 (2001).
- [3] Y.L. Li and T. Ishigaki, *Chem. Mater.*, **13**, 1577-1584 (2001).
- [4] K. Zahib, K. Tatsumi, H. Abe, T. Ohsaki, Y. Sawada, and S. Higuchi, *J. Electrochem. Soc.*, **145**, 210-215 (1998).
- [5] A. Mabuchi, H. Fujimoto, K. Tokumitsu, and T. Kasuh, *J. Electrochem. Soc.*, **142**, 3049-3051 (1995).
- [6] H. Maleki, G. Deng, A. Anani, and J. Howard, *J. Electrochem. Soc.*, **146**, 3224-3229 (1999).
- [7] U. Von Sacken, E. Nodwell, A. Sundher, and J.R. Dahn, *J. Power Sources*, **54**, 240-245 (1995).